Journal of Molecular Modeling (2020) 26: 64
https://doi.org/10.1007/s00894-020-4307-x

ORIGINAL PAPER

Theoretical study of nitrogen, boron, and co-doped (B, N) armchair graphene nanoribbons

Masoud Javan[1] · Roza Jorjani[1] · Ali Reza Soltani[2]

Received: 4 November 2019 / Accepted: 22 January 2020 / Published online: 3 March 2020

Abstract

The electronic properties of the graphene nanoribbons (GNR) with armchair chirality were studied using the density functional theory (DFT) combined with non-equilibrium green's function method (NEGF) formalism. The role of donor and acceptor dopants of nitrogen and boron was studied separately and also in the situation of co-doping. The charge density, electronic density of states (DOS), and transmission coefficient at different bias voltages are presented for comparison between pure and doped states. It was found that this doping plays the main role in the distortion of the GNR lattices for cases of B and N as it affects straightly on the DOS and transmission coefficient of the systems under study. The band structure of edge was engineered by differently selecting the doping positions of B, N, and B-N hexagonal rings and it was found that there are significant changes in the electronic properties of these systems due to doping. This study can be used for developing GNR device based on doping B and N atoms.

Keywords Graphene nanoribbon · Quantum transmission · Nitrogen and boron doping

Introduction

Science moves toward the miniaturization of electronic devices and this route is limited to physical and geometrical characteristics of materials. Innovations in equipment designing and combination of new materials allow this miniaturization to be continued [1]. In two recent decades, different kinds of nanostructures based on carbon like buckyballs, nanotubes, and graphene have attracted much attention [2, 3]. Graphene is a special material because of its unique electronic properties such as linear dispersion around Dirac point and zero band gap. Some of the interesting behaviors of graphene which have been experimentally discovered make it an appropriate material for constructing electronic, magnetic, and optical devices [4, 5]. Graphene nanoribbon (GNR) is a piece of graphene which is restricted in one dimension. Electronic properties of these ribbons are dependent on width and symmetry of edges [6]. GNRs according to the shape of their edges are classified in two common groups: armchair and zigzag forms. Quantum mechanical properties of GNRs like wave function are influenced by these groups from different aspects. Wave functions related to the valence and conduction bands of zigzag graphene nanoribbons (ZGNRs) are concentrated in edges. Also edge atomic relaxation states have huge effect on their band structure properties. These edge electronic states can be adjusted by an external electric field along the width, resulting semi-metallic property. On the other hand, wave functions of the states around the Fermi level are distributed on the width for armchair type, and the effect of each atomic relaxation is too tiny [5]. According to the tight binding theory, it is understood that most of GNRs are semiconductors with a band gap which varies inversely by width, while the zero band gap of GNRs appears depending on chirality [5].

Electronic structure simulations make appropriate ways for physical and chemical study of new materials [7]. One of the convenient ways to explain and predict the electronic transport in nanoscale devices is the non-equilibrium green's function (NEGF) method combined with DFT. The validity of this method is approved by different studies under some circumstances [7, 8]. The NEGF method makes it possible to investigate the electron transport in GNRs. DFT combined with

✉ Masoud Javan
m.javan@gu.ac.ir; javan.masood@gmail.com

[1] Department of Physics, Faculty of Sciences, Golestan University, Gorgan, Iran

[2] Golestan Rheumatology Research Center, Golestan University of Medical Science, Gorgan, Iran

NEGF is used in order to consider this type of transport in open systems of GNRs [9]. These techniques are used for modeling the quantum transport characteristics in nanoelectronic devices under external bias potential [10]. According to the spin polarized DFT calculations, it is predicted that the asymmetric DOS around the edge for both valence and conduction bands of ZGNRs causes nonzero magnetic moments [3, 11, 12].

Another capability of graphite and graphene structures in nanoelectronic applications is revealed by modification of the structures using impurities, adatoms, and external field [3]. So far, graphene and GNR doping with various materials have been considered and also their properties have been studied. Ruitao and Mauricio [13] reported that hydrogen doping in semiconductor AGNR with 0.45 eV band gap can reduce band gap energy, while reversely O, N, or S doping increases band gap. Moreover, Mg and B doping eliminates the band gap and turns the GNR into the metal [13]. Rigo et al. [14] investigate transitional and electronic properties of ZGNR with Ni adsorption. They realized that Ni doping on ribbon's edges gives more stable energetic configuration than Ni doping in the middle of the ribbon. They also concluded that magnetic moments of carbon atoms at the ribbon's edges for Ni-doped case have nonzero values but these values for carbon atoms at the center of the ribbon are negligible [14]. Sevincli et al. [15] studied the effect of transition metal doping on AGNRs and their magnetic and electronic properties. They found that AGNR, which is a semiconductor, can be either a metal or a semiconductor with ferromagnetic or antiferromagnetic state as their spin moment structures depend on the width of the ribbon and the type of transition metal atom. Substitution of nitrogen or boron atom in carbon-based materials can make n or p-type doping [6]. Mukherjee and Kaloni [16] studied the electronic properties of graphene doped with N and B atoms. They pointed out that N (electron doping) and B (hole doping) co-doped can turn graphene into a semiconductor with narrow band gap. Doping in GNRs regarding their width and edge symmetry has more complex properties than doping in carbon nanotubes [6]. A GNR-based field effect transistor (GNR-FET) with adjusting width and orientation of the GNR can show the same performance as a single-walled nanotube FET [13]. Transport properties and I-V characteristics controlling the GNR under local and regular strain are considered as a future development of electronic devices. According to this fact, studying the strain effect on the electronic properties of graphene and graphene-like materials has become an important and useful field of research [17, 18]. Interestingly, some work partially similar to our research have been done before. Haung [19] investigated electronic and transport properties of B-doped and N-doped GNRs in order to achieve results on GNR-based electronic devices. He found that B-doped p-type GNR-FETs are potentially applicable. Similarly, in 2016, Varghese et al. [20] did a research on B- and N-doped GNRs in more detail. They studied structural, electronic, and energetic features of B- and N-doped GNR with different dopant atoms concentration for various configurations which ended in interesting results. In spite of all these valuable studies done until now, investigating electronic and transport properties of co-doped of B and N atoms in AGNR lattice is the difference between our job and other's work.

As we decided to do comprehensive research on AGNRs' properties, studying ZGNRs in depth is our next purpose. In this letter, we evaluate electronic and transport properties of AGNRs under the influence of B and N atoms doping with different permutations. To do that, B and N atoms are placed in different positions of a graphene lattice separately and their properties are determined. The structural properties have been investigated and the transmission curves have been drawn. In addition, simultaneous doping of B and N in AGNR lattice can give an estimate of the electron-hole interaction role in the electronic transport behavior, so B and N atoms have been doped in the considered system with different concentrations (one doped ring is added each time) at the same time. It is shown that compounds, which include B and N co-doped, possess interesting catalystic and electronic properties, making them useful for producing devices like transistors, sensors, and so on. Hence, comprehending their transmission behavior is of high significance.

Computational details

We consider electronic properties of AGNRs when boron and nitrogen doping has been applied separately and simultaneously. In order to assess the transport and electronic properties, we use the combination of two methods, DFT and NEGF formalism. Calculations are based on first principle density functional theory implemented by SIESTA code with considering solutions of Kohn-Sham equations [21]. We study related systems using the linear combination of atomic orbitals (LCAO) and considering the norm-conserving Troullier-Martins pesudopotential based on DFT approach. Structural properties of the considered systems are determined by allowing relaxation of pure and doped GNR substrate where interatomic forces (obtained from Hellman-Feynman formalism) are minimized with an accuracy of 0.05 eV/A. AGNR is placed in a supercell to avoid interactions with neighbor unitcells according to Javan et al.'s work [22]. Supercell's dimension along the A and B axes is selected 50 Å. Energy convergence criteria are imposed on 10^{-4} eV where the functional used for exchange and correlation energy fixed on generalized gradient approximation (GGA) from Perdew-Burk-Ernzerhof (PBE) presentation [23]. In the present work, the grid cutoff used is 120 Ry. The basis set used to describe valence electrons is a

double zeta polarization DZP with different cutoff radius for s, p, and d orbitals. As we expect that the long-range dispersion interactions will play a significant role in extended graphene-like systems, we used the DFT-D2 method within the PBE functional using Grimme's semi-empirical pairwise approach. Unit-cell dimensions of the AGNR selected for scattering region are $10.0 \times 23.53 \times 12.79$ Å, and Fig. 1 shows configuration features of considered AGNRs in scattering region.

For further studies, we investigate transport properties of doped AGNR systems through NEGF formalism. Green's function for each energy grid is calculated as follows:

$$G = [(E + i\eta)S - H - \sum_l - \sum_r]^{-1} \quad (1)$$

where S is the overlap matrix and simplified to I matrix for limited differences, η is a small positive number which is added to energy, and $\sum_{l,r}$ is the self-energy matrix related to right and left connections given as follows:

$$\sum = \tau g \tau^{\dagger} \quad (2)$$

where τ is the junction-device coupling matrix and g is the green's function of surface for the electrodes of the two sides of device. Density of states is given as follows:

$$DOS(E) = (i/2\pi)\ \mathrm{Tr}\ (AS) \quad (3)$$

where $A=i(G-G^t)$ and $T(E)=\mathrm{Tr}\ [\Gamma_l G \Gamma_r G^t]$. Conductance (C) at zero temperature is proportional to the transmission coefficient of electrons injected to Fermi energy, which means $C=C_0\ T(E)$ where C_0 as the quantum of conductance is obtained as $C_0=2e^2/h$ [18].

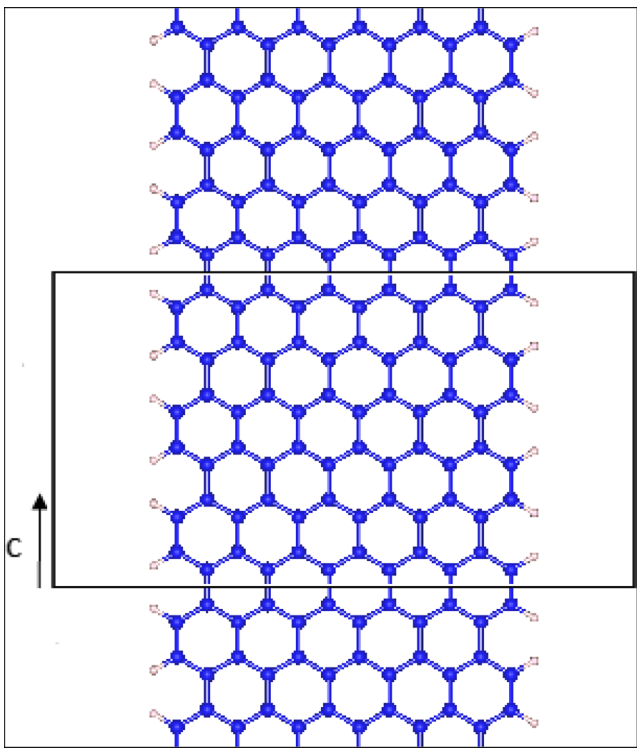

Fig. 1 Unit cell of the pure AGNR system

Results and discussion

We first study the geometrical properties of the pure and doped AGNRs. Figure 1 shows the configuration properties of considered AGNRs, including bond lengths and angle values in scattering region. For pure GNR, the H-C bond length is 1.09 Å, and the C-C bond length in the middle and also at the edges of the ribbon is approximately equal to 1.42 Å which is in good agreement with experimental value of 1.421 Å [24]. Honeycomb network can be seen for pure AGNR's with precise bond angle of 120°. Considering that perfect hydrogen terminated AGNR, we have shown its electronic density of states in Fig. 4a. As we can see, the considered AGNR has a band gap of about 0.5 eV with asymmetric contribution of electron density of states around zero energy. This situation indicates that the DOS of valence and conduction bands of hydrogen which terminated AGNR are not the same, unlike the situation for pure armchair graphene. This result is in good agreement with recent studies [5, 17].

On the one hand, many possible and different positions can be opted for B and N doping in the system that may show various behaviors. We distinguish these possibilities by determining "*cis*" and "*trans*" structures [25]. On the other hand, transition from graphene state to boron-nitride graphene nanosheets with high amount of impurities have been studied by increasing the number of (B, N)-rings. For the study of the role of B-doped on the electronic structure of AGNR system we have doped B in different scheme on AGNR sheet. Figure 2a shows the bond length and angle values for B-doped structures. B1 indexed system illustrates one B atom doping in the middle of the ribbon. For both "*cis*" and "*trans*" structures, the B-C bond length is 0.1 Å shorter than experimental value of STM measurement [25]. In this case, the range of B-C length varies around 1.48 Å with deviation of about 0.01 Å. In bonds near atom B, as it can be seen, the B-C bond length has slight increase of about 0.06 Å in comparison with C-C bond length which is related to the higher value of B atomic radius. The same bond length was previously reported for boron carbide compounds which refer to π-bounding between B and C atoms [26, 27]. Meanwhile, C-C lengths are slightly screwed at the edges as the C-C lengths differ from 1.38 to 1.43 Å. It is worthy to know that doping makes distortion in angles from the original value of 120°, consequently, may create strain in graphene lattice. In the B1 doping states, the small deviation of C-C bounds makes an angle of 117° between $\widehat{CCH}$ at the edges which expands distortion to the lattice of the GNR.

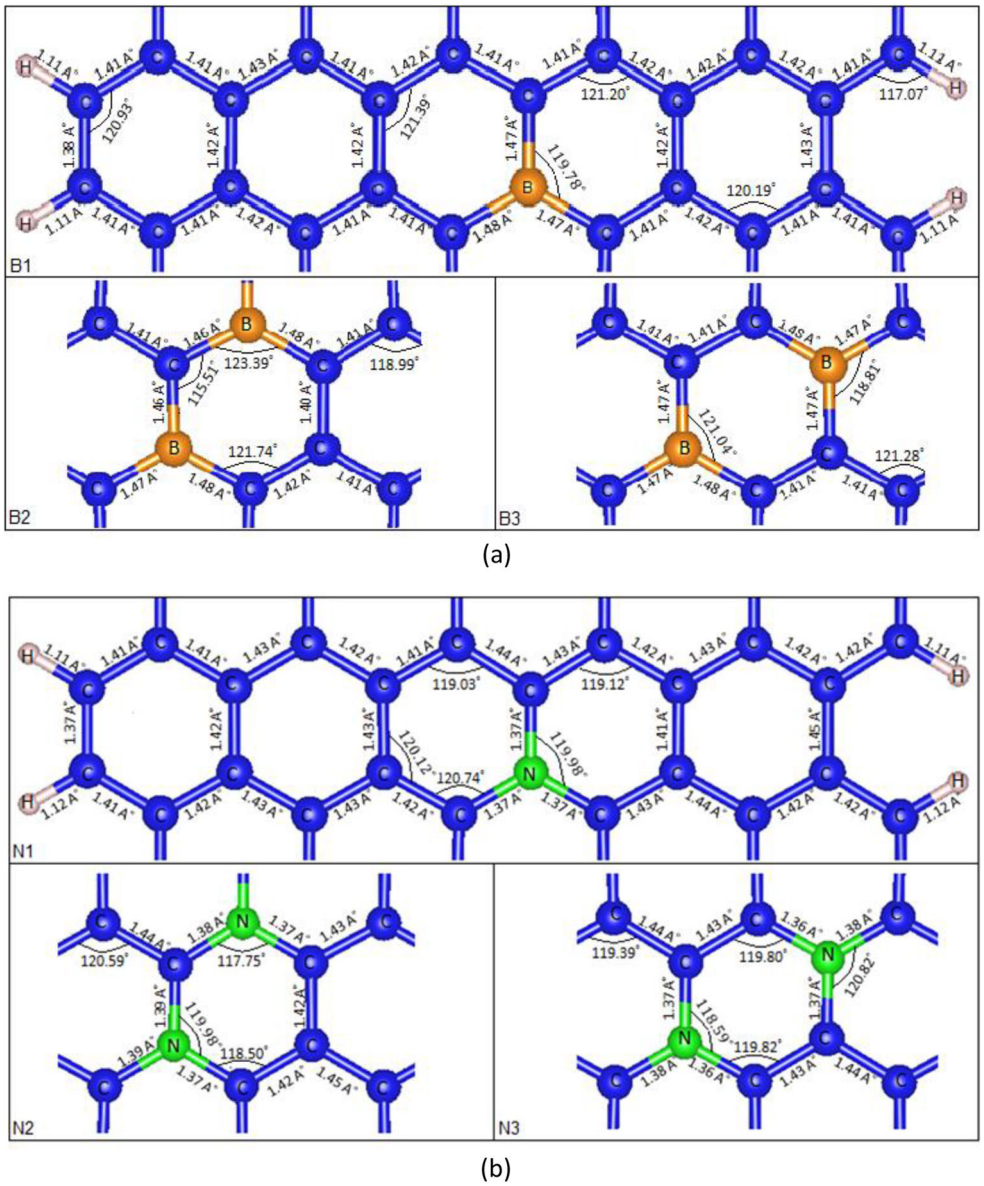

Fig. 2 Bond length and angles for **a** B-doped AGNR. **b** N-doped AGNR. **c** AGNR with co-doped B and N atoms. **d** A number of AGNRs with different number of fully co-doped B-N rings

B2 and B3 indexed systems refer to the "*cis*" and "*trans*" structures of B-doped AGNR. The distance between two B atoms is 2.47 Å for "*cis*" and 2.86 Å for "*trans*" states. The length of B-C is about 1.47 Å, and the C-C length at the edges varies around 1.37 Å. In fact, our results are in good agreement with theoretical research [25, 26].

In the same manner, Fig. 2b displays structural features of three different ways of N doping in the AGNR systems. In N1 indexed system, there is only one N atom doped in the middle of the ribbon. While, N2 and N3 indexed systems point to the "*cis*" and "*trans*" structures of N-doped AGNR.

There is a remarkable change in bond angles whether in the middle of the ribbon or on the edges, indicating that doping makes distortion in the lattice. The C-C bond length surrounding B-dopants have remarkable reduction in comparison with normal C-C bonds. Whereas, this situation is reverse for N doping. The main reason for such difference is the electrostatic origin of B-C and N-C bonds as B is a donor and N is an acceptor, and this trend happens also for N2 and N3 indexed systems, as well as for B2 and B3.

Figure 2c presents structural properties for three different types of one B and N atom doping simultaneously in the GNR. Structural features for three different types of B-N doped rings from six considered types are shown in Fig. 2 (d). At this point, firstly a ring including B and N atoms were doped in GNR, then one more ring was added to the previous state each time, and finally there is a row of B and N atoms in the ribbon. The length of B-N bonds is from 1.43 to 1.46 Å where the bond angles are 120° as the honeycomb flat structure remains in stable state. The B-H and N-H bonds length at edges for BN8 and BN9 are 1.03 Å and 1.22 Å, respectively. Mulliken charge population shows that in the N atoms a

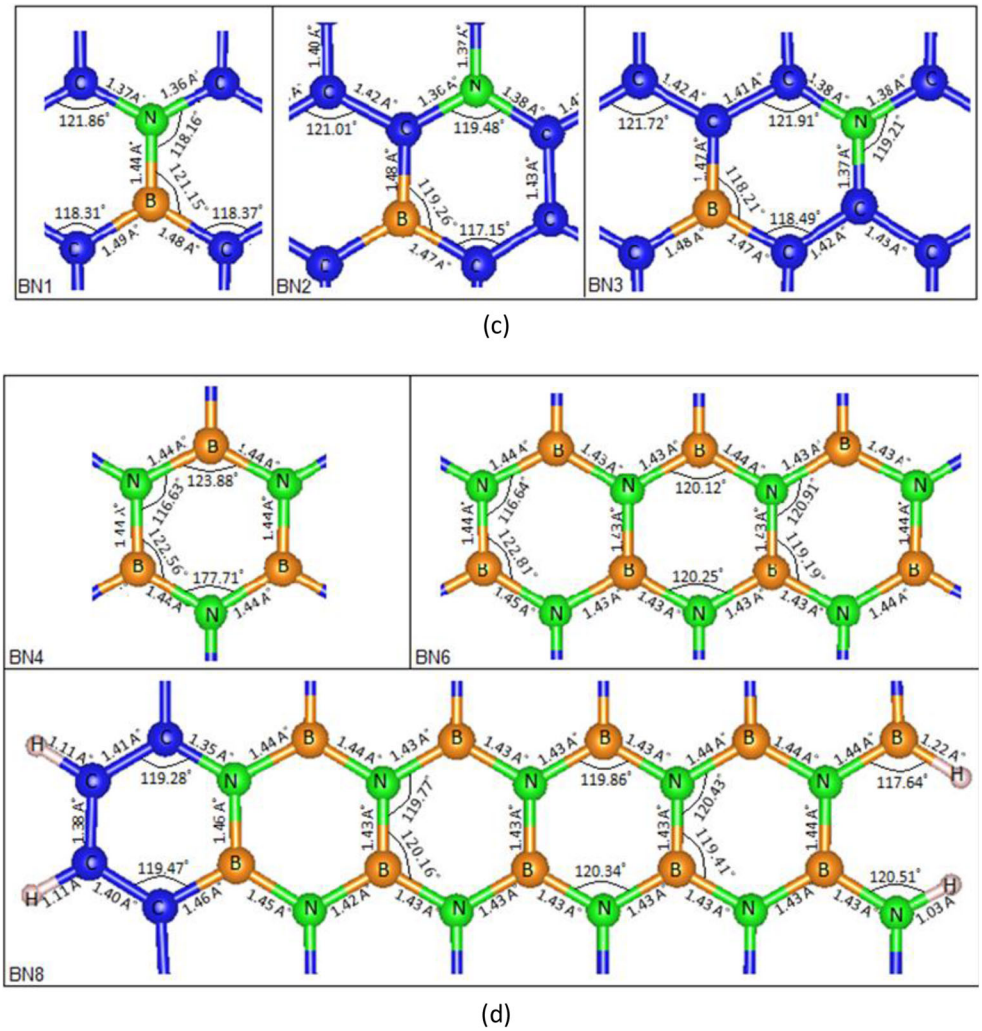

Fig. 2 (continued)

negative charge varies between −0.35 and −0.45e which shows that the N atoms are acceptors. In a different situation, the B atoms are donor while their charge varies between +0.05 and + 0.15e in different systems under study.

Relative binding energy per atom for all the studied systems is shown in Fig. 3. The binding energy can be defined as a difference between total energy of the conformed and isolated systems in the unit of the number of atoms in the system. In general, binding energy grows about 0.05 eV with doping of B and N atoms. In the same way, binding energy for the single type doped systems is almost equal. In case of co-doped systems, binding energy rises remarkably with the increase of BN rings, and binding energy grows about 0.30 eV more than pure AGNR.

For further study, we discuss the electronic structure of the considered systems. Figure 4 shows total and projected DOS for the considered doped AGNR structures. Density of states related to B and N atoms are shown in red and green colors. Figure 4a illustrates DOS for pure AGNR which has a band gap of 0.6 eV and three main peaks around − 3.25, − 1.9, and 2.1 eV. As shown in Fig. 4b (B-doped AGNR) and Fig. 4c (N-doped AGNR), the peak positions change, especially the first peak in B1 rises strongly more than two times of the pure

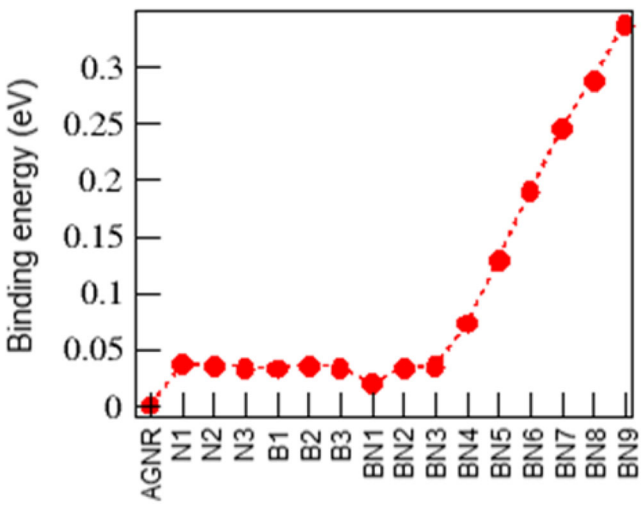

Fig. 3 Binding energy for all the considered systems

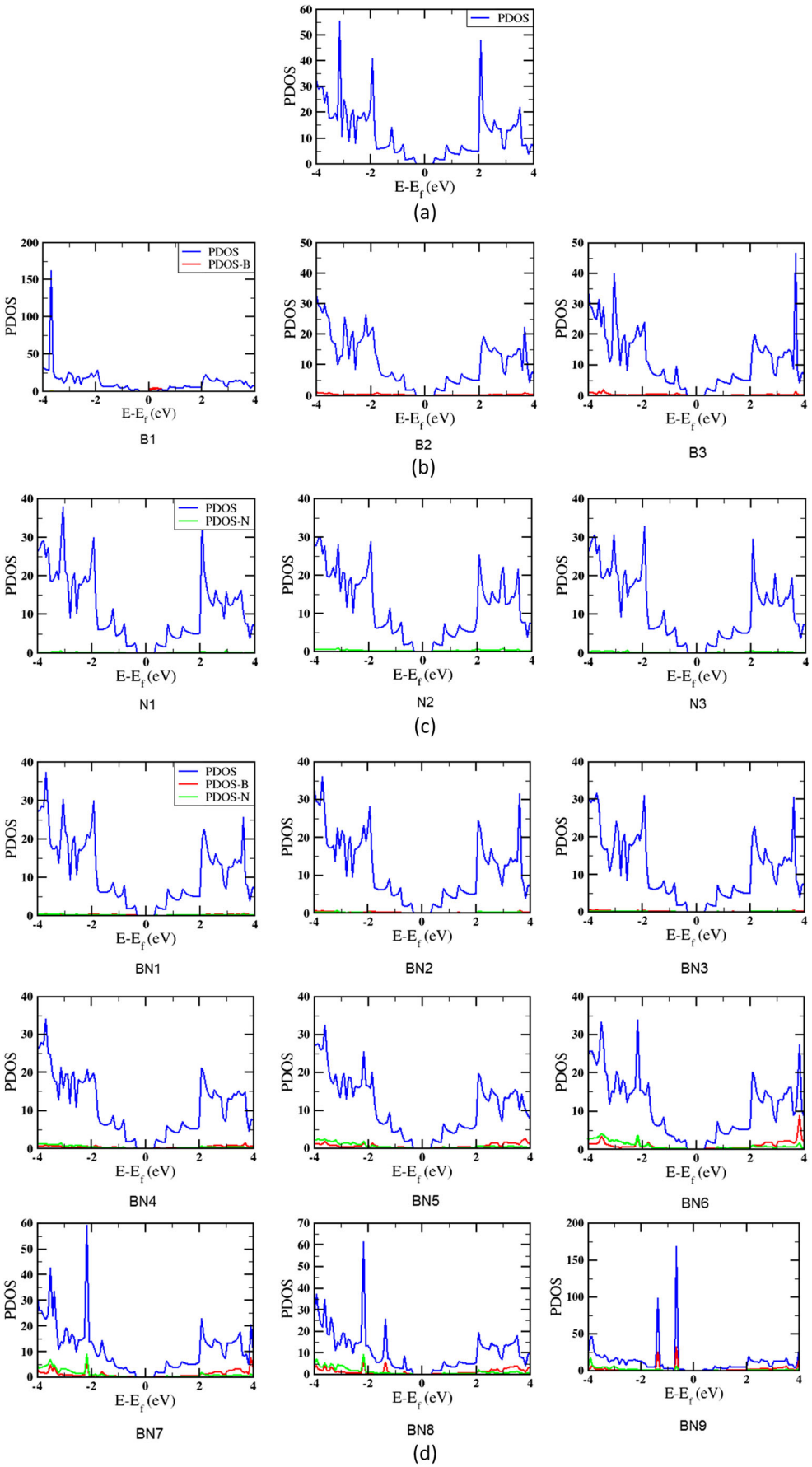

Fig. 4 DOS for **a** pure, **b** B-doped, **c** N-doped, and **d** BN-doped AGNR

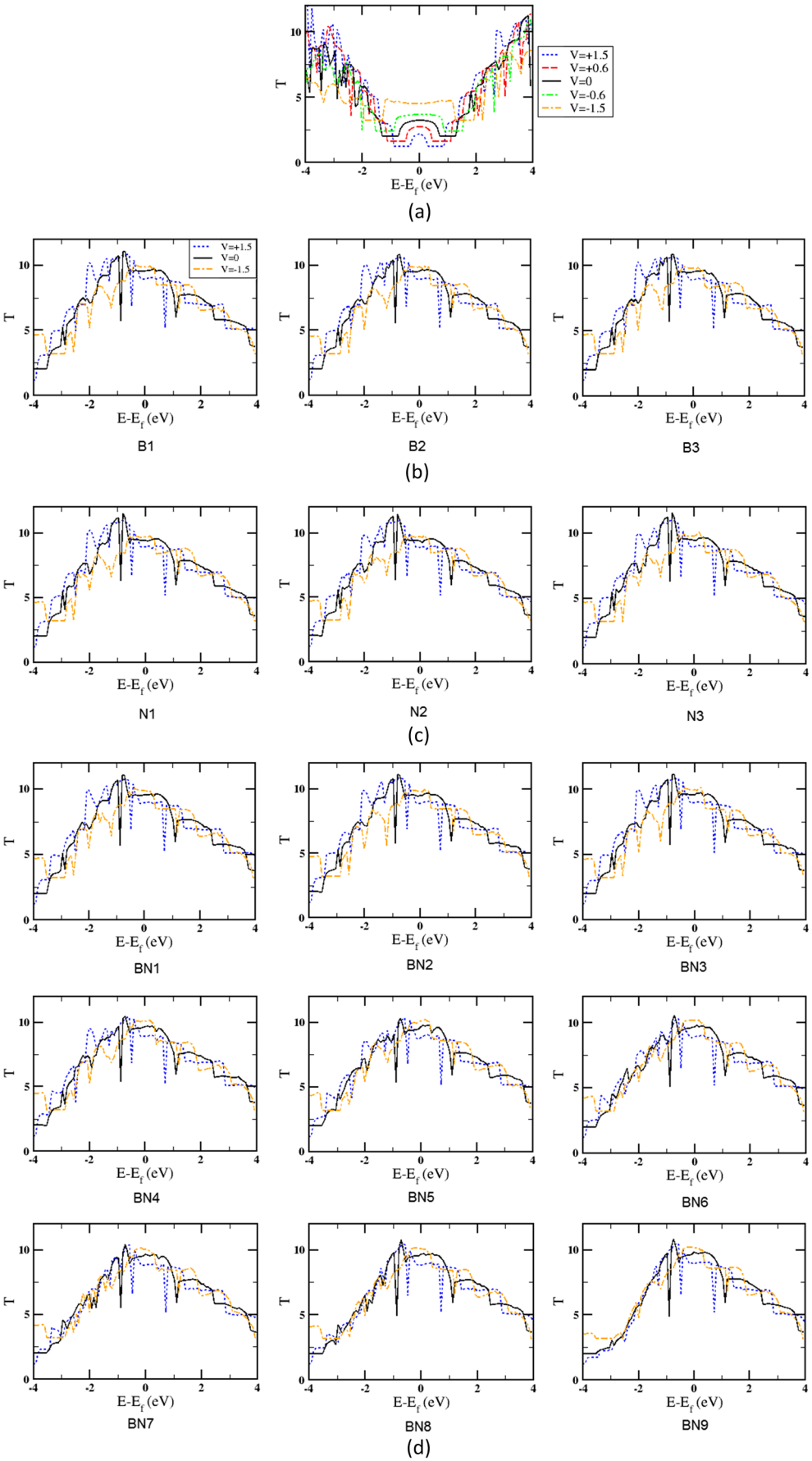

Fig. 5 Transmission for **a** pure GANR, **b** B-doped GANR, **c** N-doped GANR, and **d** BN-doped GANR

corresponding peak. In addition, Fig. 4b implies that the band gap is mostly unchanged, but valence and conduction band are altered which can affect quantum transport of electrons and holes accordingly. By considering Fig. 4c, we can see no significant change in band gap with N doping. Changes in valence and conduction bands are remarkable at – 4–4 eV where these changes in the electronic structure of AGNR are based on N-P orbital hybridization with carbon atomic orbitals.

The effect of different types of co-doped (B, N) on the electronic structure of AGNR is presented in Fig. 4d which still has no great impact on the band gap, but many changes happen for valence and conduction band. Also, density of states is much affected near the band gap for these systems. A remarkable difference with single doping can be seen in BN9 which is the existence of two sharp peaks at − 0.6 and − 1.3 eV in the valence band which exist in the other system samples but in lower density of states.

For more studies around electronic structure of the AGNR doped systems with B, N and co-doped (B, N), we have investigated the transmission coefficient (T(E)) of these systems separately. First of all, we have studied pure AGNR system T(E) where we applied different voltages. As it is shown in Fig. 5a, the solid black line shows the transmission coefficient at zero bias for the pure AGNR which has a constant value around Fermi level. Given that the transmission coefficient describes the probability of an electron tunneling between junctions, so we can conclude a constant probability of electron tunneling at zero bias in range the of − 0.5–0.5 eV. Far from Fermi level, we have a step-like growth of the transmission coefficient which is compatible with the raise of the electronic density of states of pure AGNR.

At forward bias, we can see a decrease of transmission coefficient as the voltages grows. At reverse bias with switching on − 0.6 V, the transmission slightly increases around zero energy and with the growth of the reverse bias to − 1.5 V the transmission shifts up more than twice. The fluctuation around pure state transmission coefficient varies in different forward bias, where at negative energies the T-coefficient drops slightly.

In Fig. 5b, we have shown the transmission coefficient of B-doped AGNRs for all considered configurations of the study. As we can see, the transmission coefficient increases suddenly around Fermi level in comparison with pure AGNR and in the range of – 2–2 eV. The same situation can be seen for N and co-doped (B, N) systems in Fig. 5 c and d, respectively. In the comparison between B and N-doped AGNR systems, it is found that some parts of T-coefficient fluctuations are more intensive than the other one, and also the intensity of T coefficient for N-doped systems is slightly larger than B-doped case. For both B and N-doped systems, the "*cis*" and "*trans*" structures show approximately the same behavior and there is no effective sensitivity to the dopant positions. However, for (B, N) co-doped systems, we can see significant change in T(E) curves with the increase of the BN rings, as T(E) becomes smooth and fluctuations decrease specially at –4–4eV. In all constant systems, the role of the forward and reverse bias voltage remains the same as the behavior of pure AGNR.

In order to consider further electronic features of the considered system with the highest amount of doping, the effects of the electronic field on BN9 indexed structure are shown in Fig. 6 in order to investigate the role of electronic field on the studied structures. The yellow and red points represent the negative and positive charge concentration positions, respectively. Figure 6a relates to the zero bias and Fig. 6b to the 1.5 V bias. As it is obvious in the figure, electronic field causes creation of polarization in the region of C-C, B-B, N-N, B-N, B-H, and N-H bonds. This polarization can change the electronic structure of AGNRs so that it causes relative decline of transmission coefficient in transmission curve for BN9 case especially in the region of positive energies.

Figure 7 shows the band structure of BN9 indexed system in the presence and absence of electronic field with equivalent voltage of V = 0 and 1.5 eV. Band structure is plotted along the G-Z direction of the Brillion zone. Energy gap for the BN9

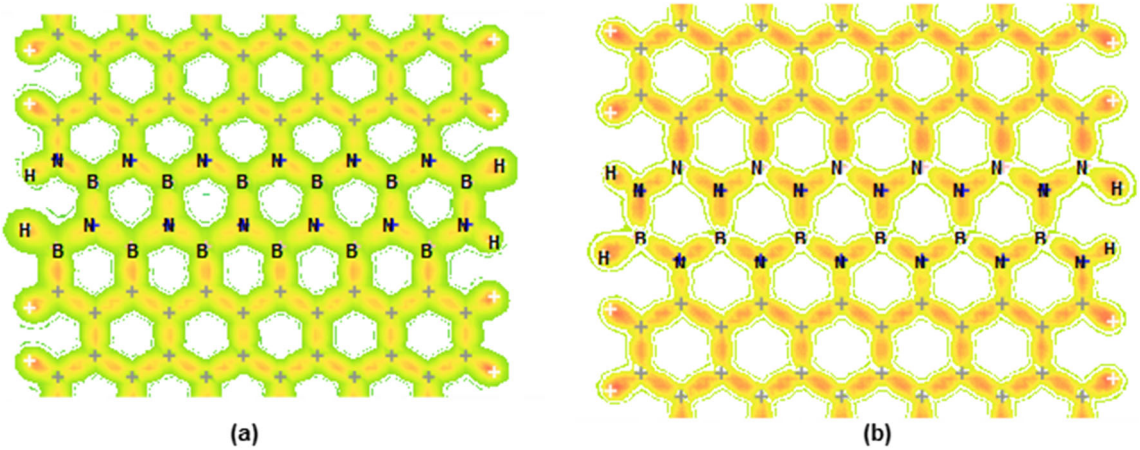

Fig. 6 Charge density for BN9 indexed system

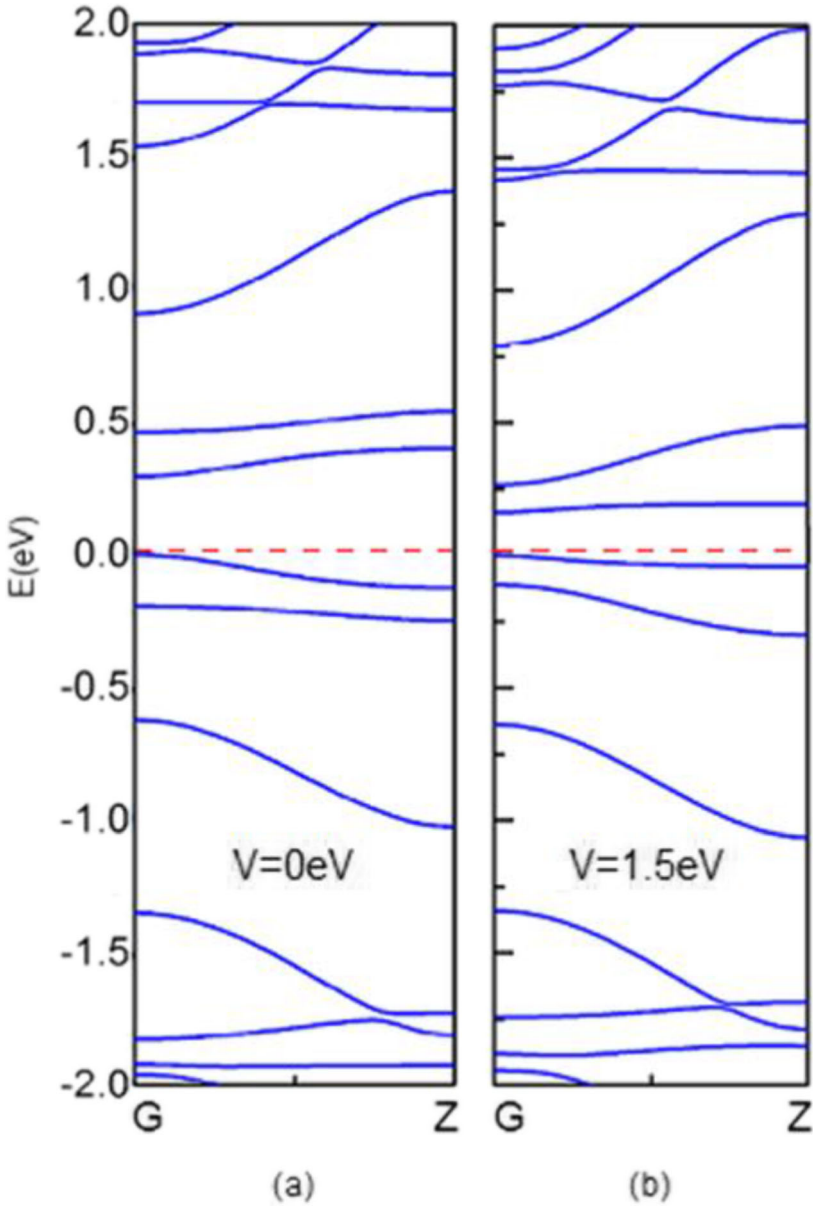

Fig. 7 Band structure for BN9 indexed system

system in the absence of electronic field is equal to 0.29 eV and it decreases to 0.16 eV by applying the electric field. Generally in all the mentioned samples, energy gap decreases with the voltage increasing and valence and conduction bands near the Fermi level have changed under effect of the applied electric field. There is a significant change in the π^* states of conduction band where π and π^* are made from B, N and C atoms p-orbitals hybridization. Also electric field has little effect on band structure in the energy range of more than ±0.5*eV*.

Conclusions

The electronic properties of the doped armchair graphene nanoribbons (GNR) with single type B and N atoms and co-doped (B, N) atoms were studied due to the density functional theory (DFT) combined with non-equilibrium green function method (NEGF) formalism. The role of donor and acceptor dopants of the boron and nitrogen was studied separately and in the situation of co-doping states. It is found that doping has a main role in the distortion of the GNR lattices for cases of B and N as it affect straightly on the DOS and transmission coefficient of the considered systems. Mulliken population charge (MPA) analysis shows that the N atoms have a negative charge which varies between −0.35e and −0.45e which shows that the N atoms are acceptors. In a different situation, the B atoms are donors while their charge varies between +0.05e and +0.15e in different systems under study. In cases of co-doped systems, binding energy rises remarkably with the increase of BN rings, and binding energy grows about 0.30 eV more than pure

AGNR. The charge density, electronic density of states (DOS), and transmission coefficient characteristics are presented for comparison between pure and doped states. We found that the changes in valence and conduction bands are remarkable at – 4–4 eV where these changes in the electronic structure of AGNR are based on N-P orbital hybridization with carbon atomic orbitals. The band edge can be altered through different selection of the doping positions as it significantly changes the electronic properties of the system.

References

1. Yan Q, Huang B, Yu J, Zheng F, Zang J, Wu J, Gu BL, Liu F, Duan W (2007) Intrinsic current−voltage characteristics of graphene nanoribbon transistors and effect of edge doping. Nano Lett 7(6):1469–1473
2. Hermanson GT (2013) Bioconjugate techniques. Academic Press, pp. 627–648
3. Şahin H, Senger RT (2008) First-principles calculations of spin-dependent conductance of graphene flakes. Phys Rev B 78(20): 205423
4. Chen J, Hu Y, Guo H (2012) First-principles analysis of photocurrent in graphene P N junctions. Phys Rev B 85(15):155441
5. Raza H, Kan EC (2008) Armchair graphene nanoribbons: electronic structure and electric-field modulation. Phys Rev B 77(24): 245434
6. Biel B, Blase X, Triozon F, Roche S (2009) Anomalous doping effects on charge transport in graphene nanoribbons. Phys Rev Lett 102(9):096803
7. Brandbyge M, Mozos JL, Ordejón P, Taylor J, Stokbro K (2002) Density-functional method for nonequilibrium electron transport. Phys Rev B 65(16):165401
8. Xue Y, Datta S, Ratner MA (2002) First-principles based matrix Green's function approach to molecular electronic devices: general formalism. Chem Phys 281(2–3):151–170
9. Treske U, Ortmann F, Oetzel B, Hannewald K, Bechstedt F (2010) Electronic and transport properties of graphene nanoribbons. Phys Status Solidi A 207(2):304–308
10. Taylor J, Guo H, Wang J (2001) Ab initio modeling of quantum transport properties of molecular electronic devices. Phys Rev B 63(24):245407
11. Wakabayashi K, Fujita M, Ajiki H, Sigrist M (1999) Electronic and magnetic properties of nanographite ribbons. Phys Rev B 59(12):8271
12. Kobayashi K (1993) Electronic structure of a stepped graphite surface. Phys Rev B 48(3):1757
13. Lv R, Terrones M (2012) Towards new graphene materials: doped graphene sheets and nanoribbons. Mater Lett 78:209–218
14. Rigo VA, Martins TB, da Silva AJ, Fazzio A, Miwa RH (2009) Electronic, structural, and transport properties of Ni-doped graphene nanoribbons. Phys Rev B 79(7):075435
15. Sevinçli H, Topsakal M, Durgun E, Ciraci S (2008) Electronic and magnetic properties of 3d transition-metal atom adsorbed graphene and graphene nanoribbons. Phys Rev B 77(19):195434
16. Mukherjee S, Kaloni TP (2012) Electronic properties of boron-and nitrogen-doped graphene: a first principles study. J Nanopart Res 14(8):1059
17. Topsakal M, Bagci VM, Ciraci S (2010) Current-voltage (I–V) characteristics of armchair graphene nanoribbons under uniaxial strain. Phys Rev B 81(20):205437
18. Javan MB (2015) Electronic transport properties of linear nC20 (n≤ 5) oligomers: theoretical investigation. Physica E: Low-Dimension Syst Nanostruct 67:135–142
19. Huang B (2011) Electronic properties of boron and nitrogen doped graphene nanoribbons and its application for graphene electronics. Phys Lett A 375(4):845–848
20. Varghese S, Swaminathan S, Singh K, Mittal V (2016) Energetic stabilities, structural and electronic properties of monolayer graphene doped with boron and nitrogen atoms. Electronics. 5(4):91
21. Soler JM, Artacho E, Gale JD, García A, Junquera J, Ordejón P, Sánchez-Portal D (2002) The SIESTA method for ab initio order-N materials simulation. J Phys Condens Matter 14(11):2745
22. Javan MB, Orimi RL (2015) Electric field and phosphorus doping roles on the electronic and optical properties of SiCNanocrystals: first principles study. J Comput Theor Nanosci 12(6):1023–1029
23. Perdew JP, Burke K, Ernzerhof M (1996) Generalized gradient approximation made simple. Phys Rev Lett 77(18):3865
24. Dresselhaus MS, Dresselhaus G, Saito R, Jorio A (2005) Raman spectroscopy of carbon nanotubes. Phys Rep 409(2):47–99
25. Endo M, Hayashi T, Hong SH, Enoki T, Dresselhaus MS (2001) Scanning tunneling microscope study of boron-doped highly oriented pyrolytic graphite. J Appl Phys 90(11):5670–5674
26. Bylander DM, Kleinman L, Lee S (1990) Self-consistent calculations of the energy bands and bonding properties of B12 C3. Phys Rev B 42(2):1394
27. Bylander DM, Kleinman L (1991) Structure of B13 C2. Phys Rev B 43(2):1487